

# Development of a GPS/INS Sensor Fusion Simulation Environment Using Flight Data

Francis J. Barchesky<sup>1</sup>, Jason N. Gross<sup>2</sup>, Yu Gu<sup>3</sup>, Matthew Rhudy<sup>4</sup>, and Marcello R. Napolitano<sup>5</sup>  
West Virginia University, Morgantown, WV, 26506

This paper presents the development of a GPS/INS sensor fusion simulation environment through the use of WVU YF-22 flight data. Noise on the GPS measurements was modeled using satellite ephemeris data as well as recorded flight data. The noise characteristics of the IMU were determined from an Allan variance approach. The GPS and IMU noise models were implemented in the WVU formation flight simulator, which includes an EKF-based sensor fusion algorithm to estimate the position, velocity, and attitude of the aircraft. Using both simulated and recorded flight data, attitude estimation results were used to evaluate the accuracy of the GPS and IMU measurement noise models, since the flight data includes a high quality measurement of the roll and pitch angles from a mechanical vertical gyroscope. It was determined from this analysis that the simulator includes a realistic model of the noise present in recorded flight data, which allows for validation and analysis of sensor fusion algorithms.

## Nomenclature

$N_{sat}$	=	number of satellites
$r_x, r_y, r_z$	=	position in the local Cartesian navigation frame (m)
$V_x, V_y, V_z$	=	velocity in the local Cartesian navigation frame (m/s)
$\delta_v$	=	antenna viewing angle (deg)
$\theta$	=	pitch angle (deg)
$\theta_{ES}$	=	earth shadow angle (deg)
$\lambda$	=	longitude angle (deg)
$\phi$	=	roll angle (deg)
$\varphi$	=	latitude angle (deg)
$\chi$	=	state sigma points
$\psi$	=	yaw angle (deg)

## I. Introduction

A major benefit of employing Global Positioning System/ Inertial Navigation System (GPS/INS) sensor fusion is that an accurate navigation solution can be obtained using measurements from low-cost sensors<sup>1-6</sup>. However, without high-grade navigation sensors to act as ‘truth’ data, verifying the estimation accuracy of GPS/INS sensor fusion algorithms is difficult or impossible. To combat this conflict, the use of simulation is often employed<sup>1-4</sup>. While the use of high-fidelity simulations are the norm in the aerospace control community<sup>1-3</sup>, there is a need to develop simulators that accurately model measurement uncertainties associated in GPS and low-cost Inertial Measurement Units (IMUs) for the purpose of verifying GPS/INS sensor fusion algorithms, similarly to Redmill<sup>7</sup>.

There are multiple common approaches in modeling Micro-Electro-Mechanical-System (MEMS) IMU sensor

<sup>1</sup> M.S. Student, Mechanical and Aerospace Engineering (MAE) Department, PO Box 6106, fbarches@mix.wvu.edu, AIAA Student Member.

<sup>2</sup> Ph.D. Candidate, MAE Department, PO Box 6106, AIAA Student Member.

<sup>3</sup> Research Assistant Professor, MAE Department, PO Box 6106, AIAA Senior Member.

<sup>4</sup> Ph.D. Candidate, MAE Department, PO Box 6106, AIAA Student Member.

<sup>5</sup> Professor, MAE Department, PO Box 6106, AIAA Senior Member.

errors, such as random bias and random walk<sup>8</sup>, or Gauss-Markov processes<sup>9,10</sup>. Different noise characteristics present in a signal can be determined using an Allan variance approach<sup>11</sup>. Various authors have applied Allan variance techniques to determine noise characteristics of MEMS IMU sensors<sup>12-14</sup>. Using these techniques, a model of the noise present in IMU sensor measurements can be derived using recorded data from the sensor. This model can then be used to simulate noise within a GPS/INS simulator. Compared to IMU noise modeling, GPS noise is much more complex to model. Dong defended a M.S. thesis on the development of a GPS simulator including detailed error sources such as ephemeris, satellite clock, ionospheric, tropospheric, and multipath error<sup>15</sup>. Brown and Gerein developed an architecture for a hybrid GPS simulator<sup>16</sup>. Many other sources of GPS noise modeling exist which address various aspects of GPS<sup>17-20</sup>.

Within this paper, a Sensor Fusion Simulator (SFS) environment is developed by enhancing WVU's formation flight simulator<sup>22</sup>. Particularly, models of the measurement uncertainty associated with GPS and MEMS IMU are included. One aspect of the development of the SFS presented is that it utilizes recorded flight data for development and validation. Specifically, a GPS model is analytically obtained from GPS ephemeris data. Furthermore, the simulator is validated by comparing the simulated attitude estimation error with the estimation error exhibited using real flight data. For the case of real flight data, the attitude estimation error is monitored by comparing GPS/INS attitude estimates with measurements from a mechanical vertical gyroscope.

This paper is arranged in the following order. Section II describes the error modeling of the GPS and IMU measurements, and the sensor fusion formulation used in the validation process. Section III is the experimental setup that is being modeled. Section IV shows results of the simulation environment. Section V summarizes these outcomes.

## II. Technical Discussion

### A. Modeling GPS Measurement Errors

To develop a realistic simulation environment for GPS/INS sensor fusion, it is critical to accurately model noise present on GPS measurements. To achieve this, recorded YF-22 flight data that contained GPS measurement error parameters was utilized to derive a model of the GPS noise. The GPS measurement error parameters included the number of GPS satellites in view of the antenna, and the standard deviation of the measured position and velocity.

Upon analyzing the recorded GPS measurement error parameters, it was observed that the standard deviation of the GPS measurements followed an inverse trend as the number of satellites,  $N_{sat}$ , as shown in Fig 1.

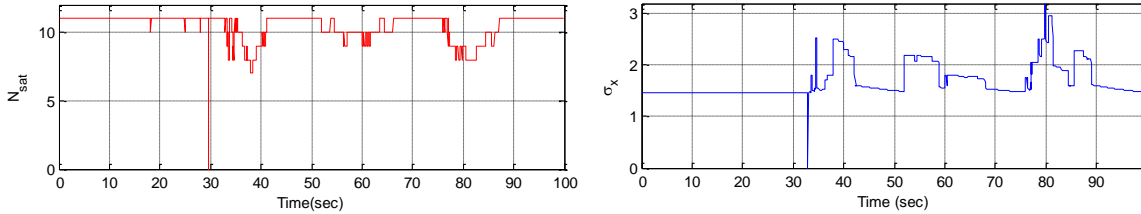


**Fig. 1: Number of Satellites ( $N_{sat}$ ) and Standard Deviation of X-position ( $\sigma_x$ )**

A linear fit between the number of satellites and standard deviation of each GPS measurement was conducted. Fig. 2 shows the z-position standard deviation linear fit. Both velocity and position in all directions had similar trends as Fig. 2.

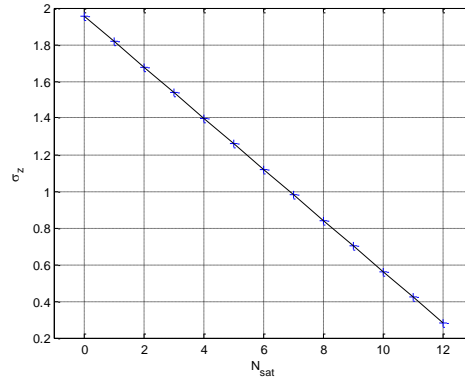


**Fig. 2: Standard Deviation of Z-position ( $\sigma_z$ ) Linear Fit**

Since the correlated relationship between the  $N_{sat}$  and the standard deviation of GPS measurements was determined, it is critical to accurately determine the number of satellites in view of the GPS receiver. Based on information about the satellite positions, the number of satellites viewable by the GPS receiver can be determined from the antenna orientation and the Earth's shadow. The satellite's position was obtained from orbital data from the National Geodetic Survey (NGS) website<sup>23</sup>. This orbital data contains each satellite's position in the Earth Center Earth Fixed (ECEF) frame, throughout a day in 15 minute increments. The GPS receiver antenna is assumed to have a viewing angle, inside of which satellite signals can be received. The orientation of the GPS receiver antenna is obtained from the attitude of the aircraft.

An important consideration when looking at which satellites are viewable are the different coordinate systems used. Three different coordinate systems are used in particular. The first coordinate system is the ECEF frame. The second considered coordinate system is a local fixed frame, given in a North East Down (NED) coordinate frame with origin defined as a set point on the runway at Jackson's Mill, WV, which is the test location used for WVU Flight Controls Research Lab (FCRL) flight testing. The third coordinate frame used is the aircraft body coordinate (ABC) frame, which is fixed to the aircraft. The important relationships between these coordinate frames are given by the following rotation matrices<sup>8</sup>:

$$\begin{bmatrix} x \\ y \\ z \end{bmatrix}_{NED} = \begin{bmatrix} -\sin \varphi \cos \lambda & -\sin \varphi \sin \lambda & \cos \varphi \\ -\sin \lambda & \cos \lambda & 0 \\ -\cos \varphi & -\cos \varphi \sin \lambda & -\sin \varphi \end{bmatrix} \begin{bmatrix} x \\ y \\ z \end{bmatrix}_{ECEF} \quad (1)$$

$$\begin{bmatrix} x \\ y \\ z \end{bmatrix}_{NED} = \begin{bmatrix} \cos \theta \cos \psi & -\cos \phi \sin \psi + \sin \phi \sin \theta \cos \psi & \sin \phi \sin \psi + \cos \phi \sin \theta \cos \psi \\ \cos \theta \sin \psi & \cos \phi \cos \psi + \sin \phi \sin \theta \sin \psi & -\sin \phi \cos \psi + \cos \phi \sin \theta \sin \psi \\ -\sin \theta & \sin \phi \cos \theta & \cos \phi \cos \theta \end{bmatrix} \begin{bmatrix} x \\ y \\ z \end{bmatrix}_{ABC} \quad (2)$$

where  $\varphi$  is the latitude,  $\lambda$  is the longitude,  $\phi$  is the roll,  $\theta$  is the pitch, and  $\psi$  is the yaw. These coordinate transformations are used in the determination of viewable satellites. First, to determine which satellites are viewable based on the antenna, the ECEF satellite positions are transformed into the ABC frame. Once in this frame, the viewable satellites are determined by which are within the antenna viewing cone (AVC), which is defined by the viewing angle of the antenna,  $\delta_v$ . For this GPS antenna,  $200^\circ$  was assumed. On the left of Fig. 3, the AVC and its relationship to the ABC and  $\delta_v$  are depicted.

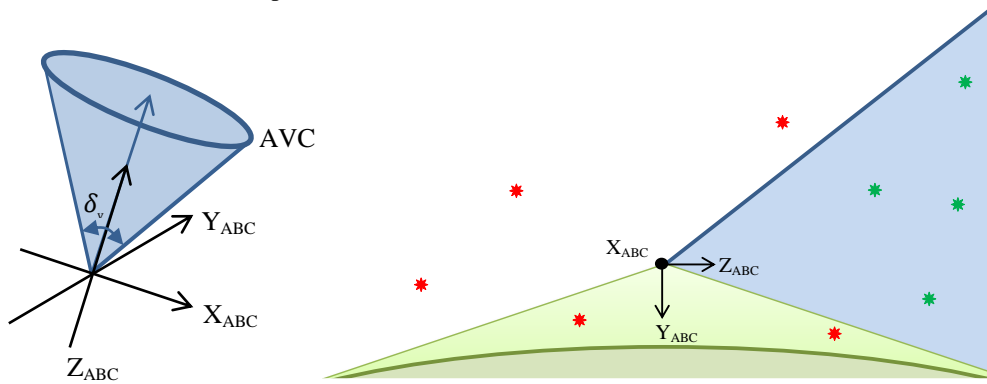


**Fig. 3: Antenna Viewing Cone and Earth Shadow**

In order to determine which satellites are viewable based on the Earth's shadow, a similar analysis is conducted. The cone of the Earth's shadow is determined as a function of the aircraft altitude. On the right of Fig. 3 the interaction between the aircraft orientation and Earth's shadow is shown. This illustration shows how when the aircraft's altitude is very low and at a high bank angle the visibility of the GPS receiver is greatly decreased. In this formulation an assumed  $3^\circ$  was added to the Earth's shadow to account for obstructions near the horizon. To determine the actual angle of the cone, the following relationship was used:

$$\theta_{ES} = \sin^{-1} \left( \frac{R}{\|r_{ECEF}\|_2} \right) + 3^\circ \quad (3)$$

where  $R$  is the radius of the Earth and  $r_{ECEF}$  is the aircraft position in ECEF coordinates.

From the attitude and altitude of the aircraft, the viewable  $N_{sat}$  can be determined. The standard deviations of the GPS measurements are determined from the viewable  $N_{sat}$  using the linear fit obtained from the flight data. Using these standard deviations, random Gaussian noise is generated in the ECEF frame. In order to implement on the GPS signals, the noise must then be transformed from ECEF to NED by Eq. (1). A block diagram summarizing the GPS noise modeling process is given in Fig. 4.

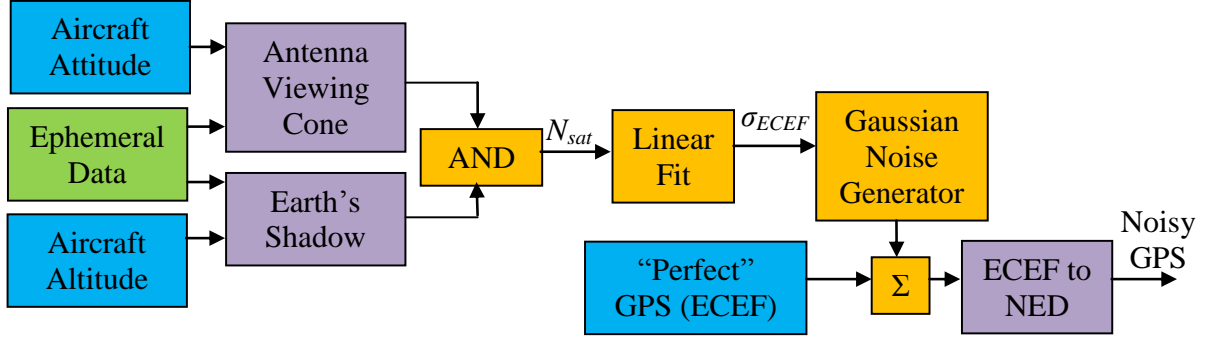


Fig. 4: Block Diagram of GPS Noise Model

In addition to this form of GPS noise modeling, it was observed in flight data that intermittent communication errors occur between the GPS receiver and general purpose computer. These errors cause a complete loss in a single sample of GPS measurements. The number of communication errors that occurred on average in the flight data was used to determine a probability of this communication drop out to occur at any sample time. At each time step in the simulation, this probability of communication loss is simulated.

## B. Modeling IMU Sensor Noise

In addition to modeling the measurement uncertainty associated with the GPS receiver, it is necessary to model typical errors associated with the IMU sensors. MEMS IMUs are inherently corrupted by many types of error sources<sup>14,24</sup>. Therefore, in order to model the dynamics associated with these sensor biases, the random walk assumption was used, which has been shown to apply to low-grade MEMS-based sensors<sup>25</sup>

$$b_k = b_{k-1} + w \quad (4)$$

where the variance of the random-noise,  $w$ , is determined based on each sensor's Allan variance as reported by the manufacturer<sup>26</sup>. In conjunction with the random walk assumption, additive white noise is also applied.

## C. 9-State GPS/INS Sensor Fusion Formulation

The 9-state loosely-coupled GPS/INS sensor fusion formulation used for this analysis was developed and used by WVU researchers<sup>27,28</sup> based upon equations derived in textbooks<sup>29-30</sup> and previous work of other authors<sup>31-32</sup>. The states of this formulation consist of the NED position  $r_x$ ,  $r_y$ , and  $r_z$ , velocity,  $V_x$ ,  $V_y$ ,  $V_z$ , and the attitude of the aircraft represented by the Euler angles,  $\phi$ ,  $\theta$ ,  $\psi$ , corresponding to the roll, pitch, and yaw angles respectively. The sensor fusion is conducted using a nonlinear state estimator with prediction and update framework, in particular, the Extended Kalman Filter (EKF). The state prediction is obtained with 3-axis acceleration and angular rate measurements from an IMU, and the measurement update is provided by NED position and velocity measurements from GPS.

# III. Experimental Set-Up

## A. WVU YF-22 Research Platform

This simulator is based on the WVU YF-22 UAV, shown in Fig. 5. The WVU YF-22 platforms have been utilized for various projects, including the validation of GPS-based formation flight control laws<sup>33-35</sup> and fault-tolerant flight control laws.<sup>36</sup>



**Fig. 5: WVU Blue YF-22 Research Platform**

The WVU YF-22 has an onboard flight computer, specifically designed for sensor fusion, consisting of an 800 MHz general purpose PC/104 and a MOD5213 micro-controller. This computer enables the collection of measurements from the following: GPS receiver, digital IMU, mechanical gyroscope, SpaceAge Control® nose probe, surface deflection potentiometers, and pilot commands. All peripherals are connected through a custom printed circuit board, shown in Fig. 6. The GPS receiver is a Novatel® OEM4 which is configured to provide the best available Cartesian position and velocity (BESTXYZ Packet<sup>37</sup>). The GPS solution is updated at a rate of 20 Hz. The digital IMU is an Analog Devices® Intelligent Sensor (ADIS) 16355 temperature compensated tri-axis IMU which provides data from rate gyroscopes and accelerometers at 50 Hz. The mechanical gyroscope is a Goodrich® VG34 which provides ‘truth’ data of the pitch and roll angles and is recorded at 50Hz.



**Fig. 6: Custom Printed Circuit Board**

## IV. Results

### A. GPS Noise Modeling

To demonstrate the effectiveness of the number of satellite modeling implemented in the simulator, the left of Fig. 4 shows the viewed  $N_{sat}$  in both simulation and recorded flight. The right of Fig. 7 is a histogram of the viewed  $N_{sat}$ , which shows the distributions of the simulation and recorded flight data. These figures illustrate the similarity between the simulated number of satellites and the number of satellites viewed from flight data, thus providing some verification of the model. Also the histogram of the comparison reveals that the model simulates lower numbers of satellites more often than in the flight data, therefore the simulation provides a more conservative model than actual flight data.

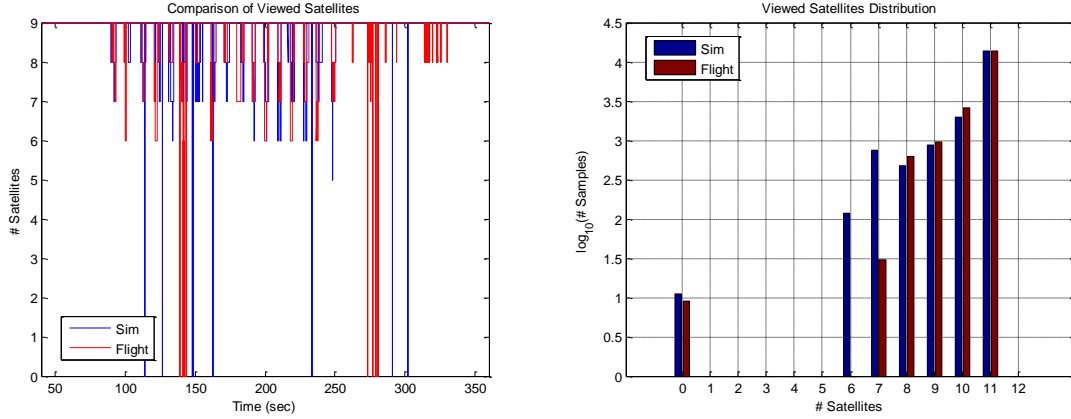


**Fig. 7: Simulated and Recorded Number of Viewed Satellites**

From the attitude and location of the aircraft the viewable  $N_{sat}$  can be determined. The viewable  $N_{sat}$  and the linear fit, which was approximated from flight data, produce the standard deviation of the GPS measurements. Using these standard deviations, random Gaussian noise is generated in the ECEF frame. In order to implement on the GPS signals, the noise must then be transformed from ECEF to NED by Eq. (1).

## B. Sensor Fusion Simulation Environment

The simulation environment is quantitatively evaluated by comparing attitude estimates from recorded and simulated flight. The simulation and recorded flights were of a single lap of the YF-22. Tables 1 and 2 reveal the attitude estimation performance of seven recorded and simulated flight laps:

**Table 1: Recorded Flight Lap Estimation Performance**

Recorded Path #	Pitch Angle (deg)		Roll Angle (deg)	
	Mean Absolute Error	Error Standard Deviation	Mean Absolute Error	Error Standard Deviation
1	2.80	1.65	1.27	1.53
2	2.22	1.36	1.47	1.65
3	2.76	1.55	1.62	1.94
4	3.06	2.15	1.27	1.57
5	2.05	0.97	1.56	1.88
6	2.40	1.10	1.75	2.02
7	2.84	1.21	1.01	1.17
<b>Mean</b>	2.59	1.43	1.42	1.68

**Table 2: Simulated Flight Lap Estimation Performance**

Simulation Path #	Pitch Angle (deg)		Roll Angle (deg)	
	Mean Absolute Error	Error Standard Deviation	Mean Absolute Error	Error Standard Deviation
1	0.99	0.79	0.50	0.68
2	2.38	2.27	1.79	2.46
3	1.16	1.40	1.44	1.30
4	1.01	1.27	1.78	1.50
5	1.29	1.09	1.10	1.42
6	1.13	1.49	1.98	1.90
7	2.93	2.22	2.09	2.54
<b>Mean</b>	1.55	1.50	1.53	1.68

From the above Tables 1 and 2 the largest difference between the simulated and recorded flight data estimation performance is in the pitch angle. The differences between the mean absolute errors can be contributed to the following reasons: misalignment between the vertical gyroscope and IMU due to mounting, uncertainty in the leveling of the vertical gyroscope, level arm correction between the vertical gyroscope and GPS receiver is not included into the simulation environment. The differences between the standard deviation could be contributed to the slightly conservative number of satellites modeling, as well as additional disturbances which can occur in real flight, such as wind turbulence effects. Due to the overall comparison of the estimation performance, the GPS and IMU noise modeling can be assumed an adequate approximation of these sensors characteristics.

## V. Conclusions

This paper presented the development of a simulation environment through the use of flight data. First, an accurate model of noise in GPS was determined using a combination of orbital and flight data. The number of viewable satellites was obtained by utilizing orbital data, and the position and attitude of the aircraft. Linear relationships were determined from flight data between the number of viewed satellites and the standard deviations of the GPS measurements. Next, the IMU noise was modeled as random walk and additive white noise through the use of the manufacturer's reported Allan variance. The GPS and IMU noise models are implemented in the YF-22 flight simulator. Lastly, an attitude estimation comparison was conducted between the simulator and real flight data. The similarity in the estimation performance demonstrates the effectiveness of the model in simulating realistic sensor errors. The development of this simulator allows for more realistic testing and evaluation of GPS and MEMS sensor fusion algorithms for use in flight applications.

## Acknowledgments

This research was partly funded by NASA grant # NNX07AT53A and grant # NNX10AI14G.

## References

- <sup>1</sup> Kaplan, E., Hegarty, C. *Understanding GPS Principles and Applications*. 2nd ed. Arttech House. Norwood, MA, 2006.
- <sup>2</sup> Crassidis J. L., "Sigma-Point Kalman Filtering for Integrated GPS and Inertial Navigation," *AIAA Guidance, Navigation and Control Conference and Exhibit*, San Francisco, CA, 2005.
- <sup>3</sup> Wan, E., van der Merwe, R. "The Unscented Kalman Filter for Nonlinear Estimation" *Proceedings of the IEEE Symposium (AS-SPCC)*, Lake Louise, Alberta, CA, Oct., 2000.
- <sup>4</sup> van der Merwe, R., Wan, E. and Julier, S., "Sigma-Point Kalman Filters for Nonlinear Estimation and Sensor Fusion- Applications to Integrated Navigation." *AIAA Guidance, Navigation and Control Conference*, Providence, RI, 2004
- <sup>5</sup> Mammarella, M.; Campa, G.; Napolitano, M.R.; Fravolini, M.L.; Gu, Yu.; Perhinschi, M.G.; , "Machine Vision/GPS Integration Using EKF for the UAV Aerial Refueling Problem," *Systems, Man, and Cybernetics, Part C: Applications and Reviews, IEEE Transactions on* , vol.38, no.6, pp.791-801, Nov. 2008
- <sup>6</sup> Grewal, M. S., Weill, L.R., and Andrews, A.P., *Global Positioning Systems, Inertial Navigation & Integration*, 2nd ed., John Wiley & Sons, New York, NY, 2007.
- <sup>7</sup> Redmill, K.A.; Martin, J.I.; Ozguner, U.; Tamura, K.; , "Sensor and data fusion design and evaluation with a virtual environment simulator," *Intelligent Vehicles Symposium, 2000. IV 2000. Proceedings of the IEEE* , pp.668-674, 2000.
- <sup>8</sup> Rogers, R. M., *Applied Mathematics in Integrated Navigation Systems*, 2<sup>nd</sup> Ed., AIAA, Reston, VA, 2003, Chap. 3.
- <sup>9</sup> Mao, X.; Wada, M.; Hashimoto, H.; , "Nonlinear GPS models for position estimate using low-cost GPS receiver," *Intelligent Transportation Systems, 2003. Proceedings. 2003 IEEE* , vol.1, no., pp. 637- 642 vol.1, 12-15 Oct. 2003.
- <sup>10</sup> Gaho, A.A.; Fang Jiancheng; Gul, F.; , "GPS/GLONASS/SINS Synergistic Integration into Flight Vehicle for Optimal Navigation Solution," *Mechatronics and Automation, Proceedings of the 2006 IEEE International Conference*, pp.1848-1853, 25-28 June 2006.
- <sup>11</sup> Allan, D. W., "Statistics of atomic frequency standards." *Proceedings IEEE*, s.l. : IEEE, February 1966, Issue 2, Vol. 54.

- <sup>12</sup> Xing, Z., and Gebre-Egziabher, D., "Modeling and Bounding Low Cost Inertial Sensor Errors." Monterey, CA : IEEE, 2008. IEEE/ION Position, Location and Navigation Symposium. pp. 1122 - 1132 . 978-1-4244-1536-6 .
- <sup>13</sup> Xing, Z., *Over-bounding Integrated INS/GNSS Output Errors*. The University of Minnesota. Minneapolis : s.n., October, 2010. PhD Thesis.
- <sup>14</sup> El-Sheimy, N., Hou, H. and Niu, X., "Analysis and Modeling of Inertial Sensors Using Allan Variance." IEEE Transactions on Instrumentation and Measurement, s.l. : IEEE, January 2008, Issue 1, Vol. 57. 0018-9456.
- <sup>15</sup> Dong, L., "IF GPS Signal Simulator Development and Verification," M.S. Thesis, University of Calgary, 2003.
- <sup>16</sup> Brown, A., and Gerein, N., "Advanced GPS Hybrid Simulator Architecture," *Proc. of ION 57<sup>th</sup> Annual Meeting*, Albuquerque, NM, June, 2001.
- <sup>17</sup> Langley, R. B., "GPS Receiver System Noise," *GPS World*, pp. 40-45, June, 1997.
- <sup>18</sup> Zhang, J., Zhang, K., Grenfell, R., and Deakin, R., "GPS Satellite Velocity and Acceleration Determination using the Broadcast Ephemeris," *The Journal of Navigation*, vol., 59, pp. 293-305, 2006.
- <sup>19</sup> Gustavsson, P., "Development of a MatLab-based GPS Constellation Simulation for Navigation Algorithm Developments," M.S. Thesis, Lulea University of Technology, 2005.
- <sup>20</sup> Xu, M., Su, D. K., Shaeffer, D. K., Lee, T. H., and Wooley, B. A., "Measuring and Modeling the Effects of Substrate Noise on the LNA for a CMOS GPS Receiver," *IEEE Journal of Solid-State Circuits*, vol. 35, no. 3, 2001.
- <sup>21</sup> Morton, Y. T., Zhou, Q., van Graas, F., "Assessment of second-order ionosphere error in GPS range observables using Arecibo incoherent scatter radar measurements," *Radio Science*, vol. 44, 2009.
- <sup>22</sup> Seanor, B., Campa, G., Gu, Y., Napolitano, M.R., Rowe, L., Perhinschi, M. "Formation Flight Test Results for UAV Research Aircraft Models", *Proceedings of the 2004 AIAA Intelligent Systems Technology Conference*, Chicago, IL, September 2004.
- <sup>23</sup> NGS Final Orbits [online database], URL: <http://www.ngs.noaa.gov/orbits/prod/>
- <sup>24</sup> Waegli, A.; Guerrier, S.; Skalous, J.; , "Redundant MEMS-IMU integrated with GPS for performance assessment in sports," *Position, Location and Navigation Symposium, 2008 IEEE/ION*, pp.1260-1268, 5-8 May 2008.
- <sup>25</sup> El-Diasty, M. and Pagiatakis., "Calibration and Stochastic Modelling of Inertial Navigation Sensor Errors." *Journal of Global Positioning Systems: CPGPS*, 2008, Issue 2, Vol. 7, pp. 170-182.
- <sup>26</sup> Tri-Axis Intertial Sensor with Magnetometer ADIS16405, Analog Devices, 2009. [Online]. Available: [http://www.analog.com/static/imported-files/data\\_sheets/ADIS16400-16405.pdf](http://www.analog.com/static/imported-files/data_sheets/ADIS16400-16405.pdf)
- <sup>27</sup> Gross, J., et al., "A Comparison of Extended Kalman Filter, Sigma-Point Kalman Filter, and Particle Filter in GPS/INS Sensor Fusion," *AIAA Guidance, Navigation, and Control Conference*, Toronto, 2010.
- <sup>28</sup> Jarrell, J. Gu, Y. Seanor, B., Napolitano M., "Aircraft Attitude, Position, and Velocity Determination Using Sensor Fusion", *AIAA Guidance Navigation and Controls Conference and Exhibit*, Honolulu, Hawaii Aug. 2008.
- <sup>29</sup> Roskam, J., *Airplane Flight Dynamics and Automatic Flight Controls*, DARcorporation, Lawrence, KS, 2003, Chap. 1.
- <sup>30</sup> Stevens, B. L. and Lewis, F. L., *Aircraft Control and Simulation*. 2<sup>nd</sup> ed., Wiley & Sons, New Jersey, 2003, Chap. 1.
- <sup>31</sup> Ford, T., Neumann, J., Bobye, M., and Fenton, P., "OEM4 Inertial: A Tightly Integrated Decentralized Inertial/GPS Navigation System", *Proceedings of ION GPS '01*, Salt Lake City, Utah, Sept. 2001.
- <sup>32</sup> Grewal, M. S., Weill, L.R., and Andrews, A.P., *Global Positioning Systems, Inertial Navigation & Integration*, 2nd ed., John Wiley & Sons, New York, NY, 2007.
- <sup>33</sup> Gu, Y., et al., "Autonomous Formation Flight: Hardware Development." *Mediterranean Control Conference*, Ancona, Italy, 2006.
- <sup>34</sup> Gross, J., et al., "Advanced Research Intergrated Avionics (ARIA) System for Fault-Tolerant Flight Research." *AIAA Guidance, Navigation and Controls Conference and Exhibit*, Chicago, 2009..
- <sup>35</sup> Seanor, B., et al., "3 Aircraft Formation Flight Experiment." *Mediterranean Control Conference*, Ancona, Italy, 2006.
- <sup>36</sup> Gu, Y., et al., "Design and Flight Testing Evaluation of Formation Flight Control Laws." *IEEE Transactions on Control Systems Technology*, 2006, pp. 1105-1112.
- <sup>37</sup> OEMV Family Receivers – Firmware Reference Manual; NovAtel, 2010. [Online]. Available: <http://www.novatel.com/assets/Documents/Manuals/om-20000094.pdf>